CHEMICAL ENGINEERING TRANSACTIONS
VOL. 39, 2014
A publication of AIDIC
The Italian Association of Chemical Engineering
www.aidic.it/cet
Guest Editors: Petar Sabev Varbanov, Jiří Jaromír Klemeš, Peng Yen Liew, Jun Yow Yong

ISBN 978-88-95608-30-3; **ISSN** 2283-9216
DOI: 10.3303/CET1439127

Experimental Design of Laboratory Measurements for Hydrocarbons, Salts and Dyes Adsorption on Modified Lignocellulosic Materials in Aquatic Media

George Apostolopoulos[a], Michael Fardis[a], Chryssa Chandrinou[a], Konstantinos Giannakopoulos[a], Athanasios Kontos[a], Maria Bidikoudi[a], Nikos Boukos[a], Polycarpos Falaras[a], Fragiskos Batzias[b], Dimitrios Sidiras[b], Christina Siontorou[*b]

[a]Inst. Advanced Materials, Physicochemical Processes, Nanotechnology and Microsystems, NCSR 'Demokritos', GR15310 Ag. Paraskevi, Athens, Greece
[b]Lab. Simulation of Industrial Processes, Dep. Industrial Management and Technology, Univ. Piraeus, 80 Karaoli & Dimitriou, GR18534 Piraeus, Greece
csiontor@unipi.gr

Waste lignocellulosic biomass is an abandoned agro-industrial by-product including wheat straw, barley straw, spruce sawdust, pine sawdust, corn stover, sugarcane bagasse, etc. Lignocellulosics can be used as natural adsorbents for dyes, heavy metals and hydrocarbons in wastewater, seawater, rivers and lakes. The thermochemical modification of lignocellulosic waste biomass can provide relatively low-cost adsorbents with increased sorption capacity and biodegradability, appropriate for the removal of chemicals, heavy metals and oil spills from aquatic media. This work deals with the design and performance of measurements on the surface of original and modified wheat straw and spruce sawdust adsorbents, using Brunauer–Emmett–Teller (BET) specific surface area analyser, Fourier transform infrared (FT-IR) and Micro-Raman spectroscopy. For the evaluation of microporocity of the materials, non-destructive spectroscopic techniques were used, as Liquid Nitrogen Porosimetry and Scanning Electron Microscopy (SEM), which were proved appropriate for the study of highly heterogeneous solid samples.

1. Introduction

Waste lignocellulosic biomass is natural adsorbent for dyes, heavy metals and hydrocarbons from wastewater, seawater, rivers and lakes. The thermochemical treatment (Kangwanwatana et al., 2013) of lignocellulosic waste biomass can provide low-cost adsorbents with increased sorption capacity (Bosio et al., 2014), biodegradability and appropriate for removing (i) methylene blue and other basic dyes (Sidiras et al., 2013a), (ii) hexavalent chromium (Silgado et al., 2014) and other heavy metals (Syed-Hassan et al., 2014) and (iii) diesel, crude oil (Sidiras et al., 2014) and other oil spills (Srinivasan and Viraraghavan, 2008).
Wheat and barley straw are renewable raw materials for production of cellulose, celobiose, glucose, oligoxyloses, xylose, furfural, 5-HMF, bioethanol and other chemicals (Sidiras et al., 2011a). Untreated and modified straws and sawdust are often used for removing: (i) methylene blue (Batzias et al., 2009) and other basic dyes (Sidiras et al, 2011b), (ii) hexavalent chromium (Sidiras et al., 2013b) and other heavy metals (Batzias et. al., 2012) and (iii) diesel and crude oil (Sidiras et al., 2014). In this case, the surface properties of straws play a crucial role. Since leaves and stems are the main components of straw, the surfaces of these plant parts must be considered in order to understand adsorption phenomena. The adsorption capacity depends primarily on the chemical structure of straw tissue that has direct contact with oil. The absorption capacity is a function of the structure of the straw stalks in the bundles, distances between them, the diameter and cross-sections of each stalk and leaf (Witka-Jezewska et al., 2003).

Please cite this article as: Apostolopoulos G., Fardis M., Chandrinou C., Giannakopoulos K., Kontos A., Bidikoudi M., Boukos N., Falaras P., Batzias F., Sidiras D., Siontorou C., 2014, Experimental design of laboratory measurements for hydrocarbons, salts and dyes adsorption on modified lignocellulosic materials in aquatic media, Chemical Engineering Transactions, 39, 757-762 DOI:10.3303/CET1439127

In this work the surface of wheat straw, a lignocellulosic biomass adsorbent, before and after chemical modification (e.g. by autohydrolysis), was studied under laboratory conditions, by carrying out BET surface area analysis, Raman spectroscopy measurements, FT-IR and SEM.

2. Materials and Methods

The wheat straw used in this work was obtained from the Kapareli village, close to the Thiva city at the Kopaida area in central Greece (harvesting year 2012), as a suitable source for full-scale industrial applications. The moisture content of the material when received was 8.8 %w/w; after screening, the fraction with particle sizes between 10 and 20 mm was isolated.

The autohydrolysis process was performed in a 3.75 L PARR 4843 batch reactor. The isothermal hydrolysis time was 10 min (not including the non-isothermal preheating and cooling periods). The reaction was catalyzed by the organic acids that were produced by wheat straw during autohydrolysis at a liquid-to-solid ratio of 20:1. The volume of the liquid phase (water) was 2,000 mL and the solid material dose (wheat straw) was 100 g (i.e., 91.25 g on dry basis). The stirring speed was 50 rpm. The reaction ending temperature of 200 °C was reached after 60 min of preheating (Sidiras et al., 2014)

The wheat straw was also pretreated by dilute maleic acid hydrolysis; the acid hydrolysis process was performed in the same 3.75-L batch reactor PARR 4843. The acid hydrolysis time was 0 - 50 min (not including the preheating time; preheating time must be added to these isothermal reaction time-periods to give the 'Acid hydrolysis Time'); the reaction was catalyzed by maleic acid 0.1 M at a liquid-to-solid ratio of 20:1; the liquid phase volume was 2,000 mL the solid material dose (wheat straw) was 100 g. The reaction ending temperature was 160 °C – 220 °C, reached after the 40 - 70 min preheating time-periods, respectively.

The surface areas and porosity of the powders were determined by the Brunauer-Emmet-Teller (BET) method (Brunauer et al., 1938). Liquid nitrogen isotherms at 77 K were obtained, using the Autosorb-1 MP (Quantachrome) porosimeter. Before each measurement, the samples were degassed, under high vacuum 10-5 mbar for 24 h, at 353 K in the outgassing stations of the instrument. The selected program of relative pressures covered all the pore sizes from the ultra-micropore to the large mesopores region (1×10-5<=P/Po<1).The tolerance and equilibration time of all the pressure points were set to 0 and 10 respectively. Before performing the measurements, all samples were turned into powders using a hummer mill.

The Raman spectra (Gardiner, 1989) of the samples were recorded on a Renishaw inVia Reflex spectrometer in backscattering configuration employing a near infrared (NIR) diode laser (λ =785 nm) as excitation source. Rayleigh scattering was rejected with a 100 cm^{-1} cut-off dielectric edge filter, and analysis of the scattered beam was performed on a 250 mm focal length spectrometer along with a 1,200 lines/mm diffraction grating and a high-sensitivity CCD detector. The laser intensity was 0.5 mW μm^{-2}. Subtraction of the luminescence background (%) was performed for the wavenumbers range between 120 and 1,700 cm^{-1}. Raman spectra has been performed by a polynomial fitting interpolation routine, while spectral deconvolution has been carried out by nonlinear least-squares fitting of the Raman peaks to a mixture of Lorentzian and Gaussian line shapes, providing the peak position, width, height, and integrated intensity of each Raman band.

IR spectra (Griffiths and de Hasseth, 2007) were collected on a Thermo Scientific Nicolet 6700 FTIR with N_2 purging system. Spectra were acquired using a single reflection ATR (attenuated total reflection) SmartOrbit accessory equipped with a single-bounce diamond crystal (spectral range: 10,000–55 cm^{-1}, angle of incidence: 45 ^{o}). A total of 32 scans were averaged for each sample and the resolution was 4 cm^{-1}. The spectra were obtained against a single-beam spectrum of the clean ATR crystal and converted into absorbance units. Data were collected in the range 4,000–400 cm^{-1}. Raman spectroscopy was performed in backscattering configuration employing an Ar+ ion laser (= 514.5 nm) as excitation source by adjusting the laser power to 0.1 mW /m^{-2} on a Renishaw InVia Reflex spectrometer.

The study of untreated and pretreated wheat straw samples by scanning electron microscopy (SEM) was conducted using an FEI INSPECT SEM equipped with an EDAX super ultra thin window analyzer for energy dispersive X-ray spectroscopy (EDS). The magnification was X750, X2,500, X7,500 and X20,000.

3. Results and Discussion

The BET values range from 3.0 to 7.8 m^2/g with the maximum value being received after the modification with maleic acid at 220 ºC for 50 min (Table 1). Following the analysis of the results obtained by N_2 adsorption porosimetry on untreated, autohydrolyzed and maleic acid treated wheat straw, we were able to compare the properties (BET surface area, total pore volume and mean pore diameter) for each of the

Table 1: Results derived after BET analysis of the porosimetry values obtained for the samples raw and modified wheat straw

Sample Code	Sample description	BET (m^2/g)	Total Pore Volume - TPV (mL/g)	Mean Pore Diameter - MPD (nm)
A1-WR	Wheat straw (untreated)	3.0	0.013	17.5
A2-WM-AH-200-10m	Wheat straw modified by autohydrolysis at 200ºC for 10 min	3.1	0.023	29.7
A21-WM-01M-160-30m	Wheat straw modified with 0.1 M $C_4H_4O_4$ (maleic acid) at 160ºC for 30 min	3.5	0.028	31.4
A22-WM-01M-220-50m	Wheat straw modified with 0.1 M $C_4H_4O_4$ (maleic acid) at 220ºC for 50 min	7.8	0.058	29.6

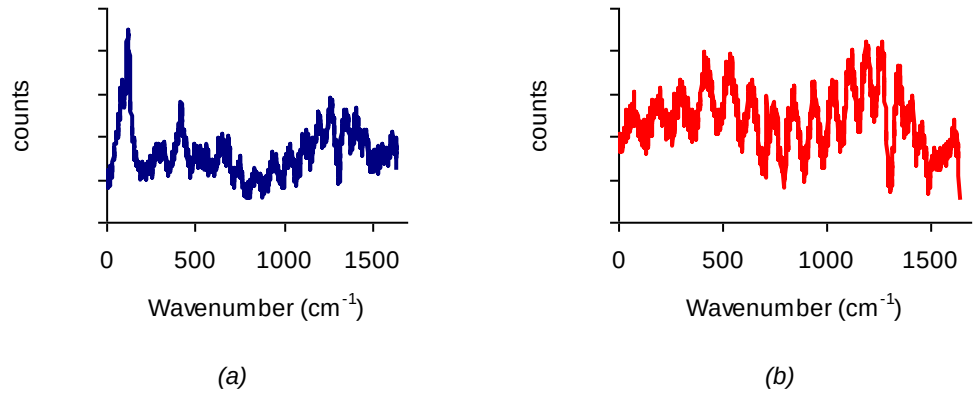

Figure 1: Raman spectra of wheat straw (a) untreated and (b) autohydrolyzed (at 200 ^oC for 10 min isothermal + 60 min preheating)

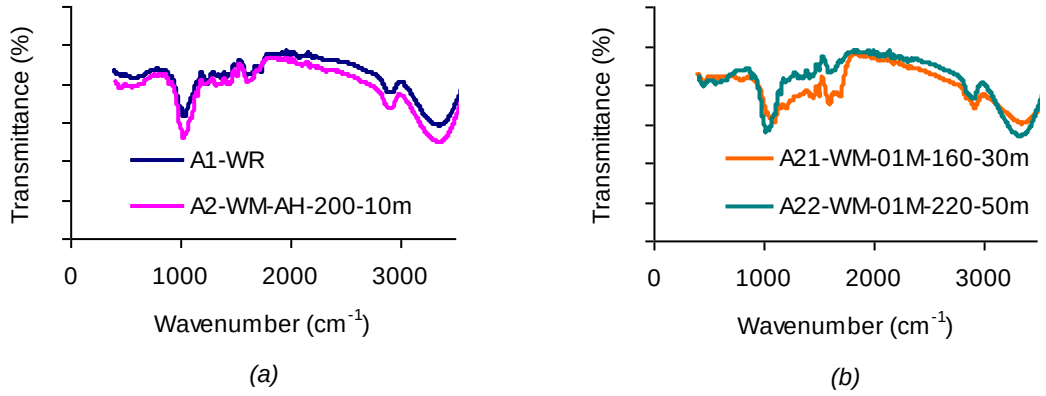

Figure 2: FT-IR spectra (a) of untreated wheat straw (A1-WR) and modified samples, autohydrolyzed at 200 ºC for 10 min (A2-WM-AH-200-10m) and (b) of modified wheat straw samples treated with 0.1 M maleic acid at 160 ºC for 30 min (A21-WM-01M-160-30 m) and at 220 ºC for 30 min 50 min (A22-WM-01M-220-50 m)

samples. It is clear that any type of treatment causes an increase in the mean pore diameter and total pore volume of the raw material. The higher value of total pore volume is observed on the materials modified with maleic acid for 50 min at 220 ºC. This treatment is the 'harsher' of the ones examined, and consequently, the one that imposes the most profound changes on the material, something that was also confirmed by Raman (Figure 1) and FT-IR spectroscopy (Figure 2). On the contrary, besides the fact that

the hydrothermal treatment (in both presence and absence of maleic acid) has an effect on the mean pore diameter, the mean pore diameter distribution does not present a certain trend. However, the values obtained for sample A2 and A22 are very similar, suggesting that the temperature at which the modification was performed is a significant factor determining this parameter, since the two modifications, although very different from one another, are both performed at very close temperatures (200 and 220 ºC, respectively).

Table 2: FT-IR peaks caused by cellulose content of untreated and modified wheat straw samples

Peak wavenumber (cm^{-1})	Bond stretching
3,420 and 3,340	OH
2,892	C-H symmetrical
1,728	C=O vibration
1,620	OH bending of absorbed water
1,510	C=C aromatic symmetrical
1,420	CH_2 symmetric bending
1,375	CH bending
1,208	C-O-C symmetric
1,152	C-O-C asymmetrical
1,108	Non symmetric in-phase ring
1,070	Skeletal C-O
1,040	C-O
1,022	C-C, C-OH, C-H ring and side group
893	COC, CCO and CCH stretching and deformation

Despite the high rate of luminescence, which makes it difficult to distinguish clearly the Raman spectroscopy peaks (Figure 1) for each component present in the samples, one can clearly notice the peaks associated with the cellulose and lignin present in both forms of the wheat. Bands at 380, 1,098, and 2,900 cm^{-1} were due to cellulose. Lignin contributions were present at 1,600 and 1,650 cm^{-1} (Agarwal and Ralph, 1997). Higher lignin concentration is responsible not only for higher peaks at 1,600 and 1,650 cm^{-1} but also for higher fluorescence background (Agarwal, 1999). Possible peaks could be present, arising from the xylose existent in the sample; however, the high luminescense does not permit us to make precise assumptions. According to Freudenberg's formula, natural lignin contains the following functional groups: metoxyl, phenolic hydroxyl, primary and secondary aliphatic hydroxyl, ketone and aldehyde groups (Sarkanen, 1987). Depending on chemical treatment, new functional groups may appear. Every lignin IR spectrum has a strong wide band between 3,500-3,100 cm^{-1}, assigned to OH stretching vibrations. This band is caused by the presence of alcoholic and phenolic hydroxyl groups involved in hydrogen bonds.This band appears in all spectrums received.

Based on literature, FT-IR spectra of lignin show no absorption bands in the 1,800-2,800 cm^{-1} wavenumber range. In accordance, in Figure 2, there is no band in this region to correspond to the lignin component of the samples. On the contrary, vibration bands at 2,920 and 2,850 cm^{-1} are attributed to lignin, specifically the C-H stretching vibrations of the methoxyl group. Absorption bands caused by stretching vibrations of carbonyl groups are usually located in the 1,600-1,780 cm^{-1} wavenumber range, while absorption bands emanating from ketone groups appear at 1,660 and 1,710 cm^{-1}. Stretching vibrations of C=C bonds appear, according to literature, in the 1,600-1,630 cm^{-1} region. In our plots, something like that is not obvious. Absorption bands located around 1,500 and 1,600 cm^{-1} are related to the vibrations of aromatic rings present in lignin. Within the spectra there are also absorption bands coming from the cellulose content in the samples (see Table 2). All these results are in good agreement with Kolpak and Blackwell (1976) findings and they were verified by the Yano et al. (1976) data found in the relevant literature.

The SEM results in Figure 3 shows rough and heterogeneous surface as regards the autohydrolysis modified wheat straw while the surface of the untreated material seems very smooth. This explains the higher methylene blue (Sidiras et al., 2011b), hexavalent chromium (Sidiras et al., 2013b), diesel and crude oil (Sidiras et al., 2014) adsorbtivity of modified wheat straw comparing to the original one.

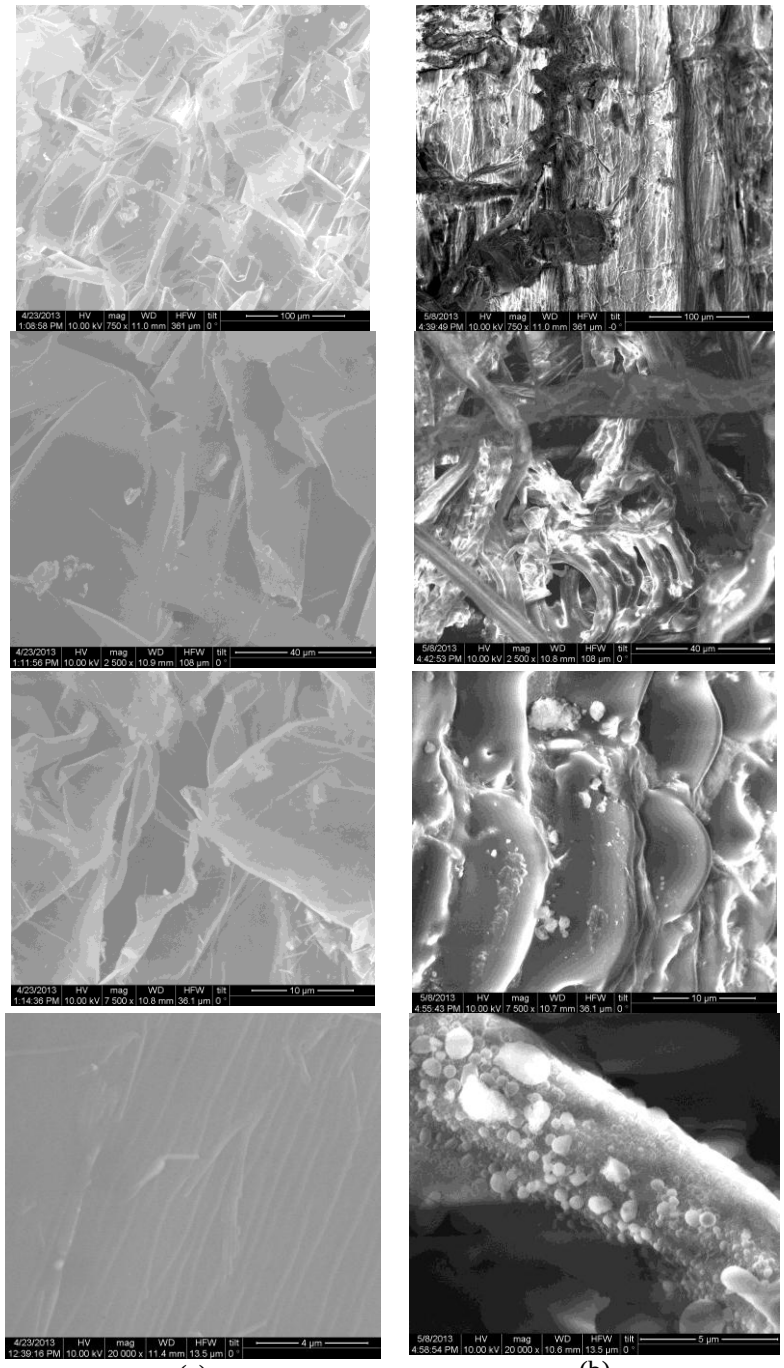

Figure 3: SEM images for the interior of wheat straw (a) untreated and (b) autohydrolyzed (at 200^{o}C for 10 min isothermal + 60 min preheating). The magnification was X750, X2,500, X7,500 and X20,000 top-down

4. Conclusions

The objective of this work was to find the surface changes of the original wheat straw and spruce sawdust due to the modification process, which lead to the improvement of their adsorption properties. The BET specific surface area analyser used for the Liquid Nitrogen Porosimetry Method facilitated the evaluation of the materials microporocity and proved the increase of the pore diameter of the modified material compared to the untreated one. The FT-IR analysis gave a significant shift of many peaks due to the modification process which increases the lignin content. The Micro-Raman spectroscopy peaks show characteristic peaks of lignin and cellulose in the untreated samples. These peaks cannot be distinguished in the modified materials. The SEM results demonstrated the highly heterogeneous surface of the modified

material comparing to the untreated one. These findings explain the significantly higher adsorbtivity of modified wheat straw comparing to the original one.

Acknowledgments

The present work is co-financed by the European Union (European Social Fund - ESF) and Greek national funds through the Operational Program "Education and Lifelong Learning" of the National Strategic Reference Framework (NSRF) - Research Funding Program: THALIS - University of Piraeus - Development of New Material from Waste Biomass for Hydrocarbons Adsorption in Aquatic Environments.

References

Agarwal U.P., Bond J.S., Miller R.B., Obst J.R., Atalla R.H., Cannon A.B., 1999. A Raman microprobe study of various anatomical features of softwoods, Abstr. Papers Amer. Chem. Soc., 217, U259–U260.

Agarwal U.P., Ralph S.A., 1997. FT-Raman spectroscopy of wood: Identifying contributions of lignin and carbohydrate polymers in the spectrum of black spruce (*Picea mariana*), Appl. Spectr., 51, 1648–1655.

Batzias F., Sidiras D., Politi D., 2012. Contribution to Tannery Waste Water Treatment for Chromium Removal/Recycle by Means of Cation Exchange Resins. Chemical Engineering Transactions, 29, 1297-1302.

Batzias F., Sidiras D., Schroeder E., Weber C., 2009. Simulation of dye adsorption on hydrolyzed wheat straw in batch and fixed-bed systems, Chem. Eng. J., 148, 459-472.

Bosio A., Rodella N., Depero L.E., Bontempi E., 2014. Rice Husk Ash Based Composites, Obtained by Toxic Fly Ash Inertization, and Their Applications as Adsorbents. Chemical Engineering Transactions, 37, 631-639.

Brunauer S., Emmett P.H., Teller E., 1938. Adsorption of Gases in Multimolecular Layers, J. Am. Chem. Soc., 60, 309-319.

Gardiner D.J., 1989. Practical Raman spectroscopy, Springer-Verlag, Berlin, Germany.

Griffiths P., de Haseth J.A., 2007. Fourier Transform Infrared Spectrometry, 2nd ed., Wiley-Blackwell, New York, USA.

Kangwanwatana W., Saiwan C., Tontiwachwuthikul P., 2013, Study of CO_2 Adsorption Using Adsorbent Modified with Piperazine. Chemical Engineering Transactions, 35, 403-408.

Kolpak F. J., Blackwell J., 1976. Determination of the Structure of Cellulose II, Macromolecules, 9(2), 273-278.

Sarkanen K.V, 1987, Lignins: occurings, formation, structure and reactions, Univ. Washington, Seattle, Washington.

Sidiras D., Batzias F., Konstantinou I., Tsapatsis M., 2014. Simulation of autohydrolysis effect on adsorptivity of wheat straw in the case of oil spill cleaning. Chem. Eng. Res. Des., In Press, dx.doi.org/10.1016/j.cherd.2013.12.013.

Sidiras D., Politi D., Batzias F., Boukos N. 2013b. Efficient removal of hexavalent chromium from aqueous solutions using autohydrolyzed Scots Pine (*Pinus Sylvestris*) sawdust as adsorbent. Int. J Environ. Sc. Technol. 10(6) 1337-1348.

Sidiras D.K., Batzias F.A., Siontorou C.G., Bountri A.N., Politi D.V., 2013a. Simulation Of Biomass Thermochemical Modification And Hydrocarbons Adsorption/Desorption. 21st Europ. Biomass Conf. Copenhagen, Denmark, 1035-1049.

Sidiras D., Batzias F., Ranjan R., Tsapatsis M., 2011a. Simulation and optimization of batch autohydrolysis of wheat straw to monosaccharides and oligosaccharides. Bioresour. Technol., 102, 10486–10492.

Sidiras D., Batzias F., Schroeder E., Ranjan R., Tsapatsis M., 2011b. Dye adsorption on autohydrolyzed pine sawdust in batch and fixed-bed systems, Chem. Eng. J., 171(3), 883-896.

Silgado K.J., Marrugo G.D., Puello J., 2014. Adsorption of Chromium (vi) by Activated Carbon Produced from Oil Palm Endocarp. Chemical Engineering Transactions, 37, 721-726.

Srinivasan A., Viraraghavan T., 2008. Removal of oil by walnut shell media, Bioresour. Technol. 99(17), 8217-8220.

Syed-Hassan S.S.A., Nor-Azemi S.N.I., Fuadi F.A., 2014. Adsorption and Dispersion of Nickel on Oil Palm Mesocarp Fiber. Chemical Engineering Transactions, 37, 709-714.

Witka-Jezewska E., Hupka J., Pieniazek P., 2003. Investigation of oleophilic nature of straw sorbent conditioned in water, Spill Sc. Technol. Bull., 8(5-6), 561-564.

Yano S., Hatakeyama H., Hatakeyama T., 1976. Effect of hydrogen bond formation on dynamic mechanical properties of amorphous cellulose. J Appl. Polym. Sc., 20(12) 3221-3231.